Journal of Engineering Research and Reports

20(9): 66-79, 2021; Article no.JERR.69966
ISSN: 2582-2926

Performance of Active Clamp and Interleaved Active Clamp Fly back DC-DC Converters for PV Systems

Noorhan E. Elsobky[1], Yasmine Ashraf[1], Mostafa A. Hamouda[1], Mohamed Sabry[1], Sahar S. Kaddah[2] and Basem M. Badr[3*]

[1]Electrical Power and Machines Department, Mansoura University, Mansoura, Egypt.
[2]Community Service and Environmental Development, College of Engineering, Mansoura University, Egypt.
[3]Technical Lead at Genesis Robotics and Motion Technologies, Vancouver, BC, Canada.

Authors' contributions

This work was carried out in collaboration among all authors. All authors read and approved the final manuscript.

Article Information

DOI: 10.9734/JERR/2021/v20i917376
Editor(s):
(1) Dr. Anuj Kumar Goel, University Institute of Engineering and Chandigarh University, India.
Reviewers:
(1) P. Abirami, Sathyabama Institute of Science and Technology, India.
(2) Ayong Hiendro, Tanjungpura University, Indonesia.
Complete Peer review History: http://www.sdiarticle4.com/review-history/69966

Original Research Article

Received 25 April 2021
Accepted 01 July 2021
Published 06 July 2021

ABSTRACT

The Flyback converter topology is a well-known and widely used for AC-DC and DC-DC power converters that cover a broad-spectrum including switching power supplies, photovoltaic (PV) system, electric cars, and fuel cell-based generation systems, and among other applications. In this work, Active Clamp Flyback (ACF) and Interleaved Active Clamp (IACF) converters are designed and simulated for the use of DC-DC converters of PV system applications. Two control systems are used to control the output voltage of the DC-DC converters for various PV conditions, which are PID (proportional integral derivatives) and FLC (fuzzy logic controller). MATLAB/SIMULINK is used to model and simulate the proposed system, where the proposed control systems are developed to regulate the output voltage for the load requirements. The simulation results of the proposed PV systems indicate that the output voltage stabilizes effectively to the required voltage (24 V) for various loads/applications while the input voltage (output from the solar panel) to the converters is varying regrading to different sun radiation levels and other parameters. The efficiency of ACF and IACF converters are found to be 88% and 90%, respectively.

**Corresponding author: Email: bbadr@uvic.ca;*

Keywords: Photovoltaic system; solar power; control systems; fly back DC-DC Converters.

1. INTRODUCTION

Nowadays, there is a significant transition from the production of fossil fuels to a more ecological and efficient approaches that involve resources such as wind or sunlight. Since people are very concerned regarding exhaustion and the environmental issues associated with traditional electricity production. Renewable energy sources have become widely used in several applications, including battery charging, light sources, and water pumping [1-4]. Such cleaner energy resources have indisputable advantages, such as low running costs (free fuel), their modular features that allow for effective capacity expansion, and carbon-free energy generation resources. Consequently, the market for photovoltaics (PV) installation is expanding, as it is perceived as one of the most innovative energy technologies [1-2].

It is often important to build and assess the production of adequate power converters to ensure optimal energy captured from solar modules along with impeccable power quality, reliability, and efficiency. This work focuses on designing DC-DC power converters for PV systems, which are based on Flyback converters. Various topologies of Flyback converters are discussed and analyzed, two topologies are proposed for PV system design, which are the Active Clamp Flyback (ACF) and Interleaved Active Clamp (IACF) topologies, as discussed in Section 2. The paper also discusses the state of art of the ACF and IACF converters for PV systems. Different control schemes and various conditions of the PV systems are investigated with respect to the system performance.

Fig. 1 illustrates the block diagram of a general solar application (PV) system. Typically, a PV system consists of solar panels, DC-DC converters, DC bus, battery charging system, and different loads. The link between both the inverters and the grid is bi-directional since the power from the grid can be used to charge the batteries and power the loads. This work focuses on designing DC-DC Flyback converters to provide DC power to the loads from a solar panel. These proposed DC-DC converters are ACF and IACF, where the IACF is generally used for feeding the harvested power from the PV to the grid. The proposed PV system for this work focuses on designing ACF and IACF converters for a solar panel, where control systems are developed for these converters for PV applications (DC load systems). These control systems are fuzzy logic controller (FLC) and proportional integral and derivative controller (PID). These converters are designed to outputs 24 V_{DC} from 17 V (output voltage from a solar panel), and the proposed control systems are used to regulate the output voltage of these converters for the loads while the output voltage of the solar panel is varying because of the variant of sun radiation levels and other parameters.

The structure of this work is described as follows. Section 1 provides the research motivation for using and designing the PV system. The methodology of this work and briefly description of Flyback topologies are provided in Section 2. The literature survey of ACF & IACF converters for PV applications is mentioned in Section 3. The design of the proposed ACF & IACF DC-DC converters and the proposed control systems (PID & FLC) are discussed by deriving the necessary analytical equations in Section 4. The simulation results of the control systems for the Flyback converters are illustrated in Section 5. Discussion of the output performance of the ACF and IACF converters are described in Section 6. Finally, the conclusions of the paper are drawn in Section 7.

2. METHODOLOGY

The methodology of this work is to design PV systems based on DC-DC Flyback converters that are suitable for the load requirements. There are various different topologies of the Flyback converters used in the literature for PV applications. This section describes the operating principles, pros, and cons of these different Flyback topologies, which concludes the proposed Flyback topologies of this PV design application. The Flyback converters are used in both AC/DC and DC/DC conversion with galvanic isolation between the input and any outputs. The conventional Flyback converter is based on a buck-boost topology with the inductor split to form a transformer, so that the voltage ratios are multiplied with an additional advantage of isolation. Flyback converters are amenable to step-down and step-up configurations, whereas the transformer acts as a magnetic energy storage device [5-6]. The conventional Flyback converter consists of a transformer, a switch in series with the primary coil, a diode in series with

the secondary side of the transformer, and an output capacitor in parallel with the load. The conventional Flyback can be designed to operate in discontinuous conduction mode (DCM) and continuous conduction mode (CCM). In the CCM, the current is always flowing in the transformer during each switching cycle. Therefore, some residual energy is always present in the transformer, so the output current has low ripple values; however, it requires a large inductance (thus a larger magnetic component), and the transfer function of the Flyback is unstable, which limits the bandwidth of the control loop and its dynamic response. In the DCM, the transformer is completely demagnetized during each switching cycle, which leads to no reverse losses in the output rectifier; however, the output current has very large ripple and thus requires larger filters [5-7]. In DCM, when the input voltage is usually low for high power circuits, the turn off losses need to be minimized by implementing the switch with some sort of turn-off snubber consisting of two primary switches, two diodes, and a snubber capacitor C_{clamp}. This topology is denoted as Flyback converter with switched capacitor turn-off snubber that is used for high current applications, one major drawback of this topology is high dissipation energy [8]. Another proposed Flyback topology in the literature for reducing the power dissipation is the ACF converter that is suitable for lower current applications, where the addition of an active clamp allows its primary switch to operate with zero-voltage switching (ZVS) thus reducing the switching loss greatly. The zero-current switching (ZCS) is considered in the operation of ACF by activating the auxiliary switch just before the primary switch. The dissipation of the stored energy in the main switch capacitance at turning on can be avoided. This reduces the voltage stress on the main switch and eliminate the DCM mode of operation; however, it increases the current stress on MOSFET switches [9-10]. On the other hand, Flyback micro-inverter with energy regenerative snubber is another topology of Flyback inverter, which can accomplish the efficiency improvement using a very simple passive snubber circuit, and a winding taken from the main power transformer. This inverter should not waste any of the energy that occurs during a switching period. This is due to the energy recovery via the auxiliary transformer winding, which is the new component added for the energy regeneration feature leading to increased performance, and transfers seamlessly along with the energy stored through the main transformer winding. Although, the snubber capacitance value must be determined large enough so that its voltage should not vary during a single switching cycle [11-18]. There are other topologies for multiple switches in Flyback, such as forward and two switch Flyback converters, where a high side MOSFET switch is added as an interim approach. The two-switch topology clamps the voltage stress on each MOSFET switch to the input voltage. The leakage energy is redirected back to the input that improves performance and eliminates the need for a dissipative snubber circuit, which is often needed in single switch converters. This converter is larger and more expensive in comparison to the conventional Flyback [19-20].

A quasi-resonant (QR) Flyback designs are used in the literature to improve the efficiency and the performance of the conventional Flyback [7]. Whereas there is a dead time or resonant “ring” in the DCM of conventional Flyback converter, because neither the diode nor the MOSFET (switch) is conducting, created by interaction between the primary inductance of the transformer and the parasitic capacitance at the switch node. The QR design adjusts the peak current and switching frequency so that the MOSFET turns on at the first “valley” of this resonant ringing and minimizes losses. Another enhancement is “valley switching”. The controller detects when the dead-time resonant ring is at its low point and turns the MOSFET on at this point to start the next switching cycle, also to reduce switching losses. The problems in the QR topology are poor transformer utilization and cross-regulation, limited to DCM or transient mode, challenging EMI filter design, limited to low to medium power levels, and the current that flows through its transformer primary side (input side) can be high, with such peak current. This results in turn-off losses that can be significant, which can be optimized further by using QR Flyback with energy regenerative snubber. The main idea behind this approach is that the current must pass via its internal body-diode just before the switch is turned on to make sure that there is no stored energy in its output capacitance when the switch is turned on so that this energy is not dissipated in the switch. This principle includes the inclusion of a few passive components and the avoidance of the use of additional active auxiliary switches. However, major disadvantages related to this topology (QR Flyback with energy regenerative snubber) are requirement of complex driver, high cost with compromised reliability performance, high generated heat from the stored energy in the

leakage, and reducing the converter efficiency. Moreover, if a higher isolation level is required the leakage inductance becomes relatively high, making the use of the snubber impractical due to the high dissipation [18-19, 21-27].

For higher power applications, the cost of providing two converters can be justified in a manner that cannot be justified for lower power applications in which Flyback based on a single switch is recommended. One of multiple converters used in the literature is IACF converters, the key principle behind IACF is to link several converters or "phases" in parallel, with each converter phase interleaved with the others. And once two converter phases are used, each one works 180° out of phase with respect to the other [28-29]. It was found that the IACF inverters have been developed and used for providing power to the grid because of the low ripple current and reasonable cost in comparison with the other multiple converters [27-29]. Among the various soft switching techniques suggested above, the ACF converter is a proper solution since it uses a simple active clamp network to achieve ZVS operation of the power switches from no load to full load, requires low magnetizing inductor and less component counts [27].

This paper focus on designing PV systems based on ACF and IACF. The advantages and disadvantages of the proposed ACF & IACF with respect to the system performance analysis for PV applications are described in Section 6. The main requirement of the proposed PV system is to provide 24 V_{DC} from a solar panel through the DC-DC power converters and the control systems. The state of the art in the field of ACF and IACF converters for PV applications is discussed in the following section.

2.1 Literature Survey

This section lists the used ACF and IACF converters for PV applications in the literature. D. P. Quesada designed and simulated an isolated AC Flyback converter (based on ACF topology) for solar power using MATLAB/SIMULINK. His design was based on maximum power point tracking (MPPT) technique, where the output voltage value was around 160 V with ripple 2% due to the dissipation losses in the components [30]. Y. H. Kim *et al*., designed and simulated a soft switching IACF system for a PV system, which consisted of an IACF converter and an unfolding bridge inverter. The IACF converter has the advantages of ZVS performance for the primary switches, reverse-recovery problem alleviation for the secondary output diodes, and small input current ripple. They used PSIM 9.0 software for the design, and the simulation results show that the ripple current was reduced, the system efficiency was improved when the electrolytic capacitor was replaced with a film capacitor [31]. P. Suskis *et al*., designed a modified Flyback converter according to the calculations for the climatic zone of Latvia for a 100 W for common mode currents in PV. They used active clamping technique with two switches, which allowed them to absorb the overvoltage spikes and skip chopping the current off and get the energy kept in the clamp-capacitor till the next cycle started. Their experimental results concluded that the ACF has lower efficiency than conventional Flyback and forward converter active clamp is the most efficient topology and has big opportunities for synchronous rectification [32]. V. Anandakumar *et al*., designed an IACF inverter based on PV systems using MATLAB/SIMULINK. They used interleaved technique in the inverter because of its advantages that are improving the reliability &

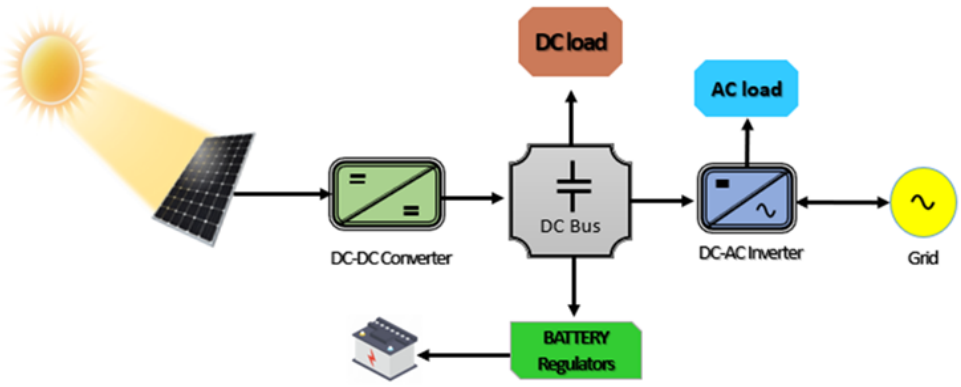

Fig. 1. Block diagram of the solar power system2.

system life and providing isolation between the PV modules and the grid line. Two Flyback converter modules with interleaved PWM were connected in parallel at the input and output sides, to reduce the ripple current on the input and output capacitors and decrease the current stress on the transformer windings [33]. S. G. Deshpande *et al*., designed and simulated ACF micro inverter to reduce voltage spike for PV applications using MATLAB/SIMULINK. The Flyback converter boosted the PV voltage to 230 V_{DC}, and unfolding the bridge converts it into grid compatible 230 AC voltage with frequency of 50 Hz and THD (total harmonic distortion) was less than 5% because of using EMI filters [34]. Y. H. Kim *et al.,* designed and simulated a soft switching IACF Inverter for a photovoltaic system using PSIM 9.0. The proposed system included an IACF converter and an unfolding bridge inverter. The simulation results of the proposed IACF showed the advantages of IACF, which ZVS performance for the primary switches, reverse-recovery problem alleviation for the secondary output diodes and small input current ripple, where the output ripple current was reduced when the electrolytic capacitor was replaced with a film capacitor [35].

2.2 Power Converter and Control Systems Designs

In this paper, ACF and IACF converters are designed for PV systems. As seen in Fig. 1, the power converters can be used to provide either AC or DC voltage to the load requirements, where these DC-DC converters are designed to provide 24 V_{DC} for load (electronic systems, charging batteries, etc.). Control systems are designed and developed to achieve the required output voltage with respect to the load requirements, which are PID and FLC control systems. MATLAB is used to model and simulate the proposed ACF & IACF systems to output 24 V_{DC} for the load. The input voltage to these converters is the output voltage from a solar panel, which is denoted as V_{in}, as illustrated in the following circuit diagrams for the proposed ACF & IACF DC-DC converters. The following subsections describe the basic operation principle of these DC-DC power converters and the control systems, whereas the derived equations are listed with respect to the design requirements of the PV applications.

2.3 Design of ACF Converter

Fig. 2 shows the circuit diagram of the ACF converter. It consists of the magnetizing inductance (L_m), leakage inductance (L_{lk}), resonant capacitor (C_r), main switch (S_{main}), auxiliary switch (S_{aux}), clamp capacitor (C_c), transformer primary turns ratio (N_p), transformer secondary turns ratio (N_s), output filter capacitor (C_{out}), secondary side diode (D), and load. The C_r should equal to the parallel combination of the parasitic capacitance of both switches [30]. The following equations are derived to calculate these components for the ACF design [30, 36].

Once the S_{main} is turned on while the switch S_{aux} is turned off. The resonant capacitor voltage across switch S_{main} is zero ($V_{Cr}(t) = 0$). The transformer primary voltage is approximately equal to input voltage (V_{in}). The secondary side diode D is turned off in this interval and the energy is stored in L_m. The clamp capacitor voltage (V_{clamp}) is equal to nV_o. When the S_{main} is turned off the parasitic capacitance of S_{main} is charged from 0 V to $V_{in}+V_{clamp} = V_{in}+nV_o$. In this time V_{Cr} is less than $V_{in}+nV_o$ so that no current flows through S_{aux} The V_{clamp} is still equal to nV_o.

Once V_{cr} equals to the addition value of the V_{in} and V_{clamp}, the S_{aux} will be turned on. The secondary side diode is still off. The energy is stored in the inductors L_m and L_{lk}, this energy charges the C_c as well in same time interval. The secondary diode D is turned on when primary voltage equals to $-nV_o$. At This moment V_{clamp} equals to $nV_o*(L_m + L_{lk})/L_m$. The energy stored in L_m is transferred to output load. The turn ratio between the transformer primary side and secondary side is equal to [30, 36]:

$$n = \frac{N_p}{N_s} = \frac{V_{in}}{V_o} * \frac{D_{max}}{1-D_{max}} \quad (1)$$

where, D_{max} is the maximum duty cycle of ACF converter. The leakage current can be calculated as [36]:

$$L_{lk} > \frac{C_r(V_{in}+nV_o)^2}{I^2_{S_{main}}} \quad (2)$$

where, $I_{S,main}$ is the peak current of the main switch. The clamp capacitor is given as [36]:

$$C_c = \frac{(1-D_{min,vin})^2}{\pi^2 L_{lk} f^2_{sw}} \quad (3)$$

where, $D_{min,Vin}$ is the minimum duty cycle as a function of the input voltage (V_{in}), f_{sw} is the switching frequency of switches. The minimum duty cycle is obtained using equation (4), the output filter capacitor can be calculated approximately as [30, 36]:

$$D_{min,vin} = \frac{D_{max} V_{min}}{V_{max,min}} \quad (4)$$

$$C_{out} \approx \frac{D_{max} \cdot P_o}{f_{sw} \cdot V_o \cdot \Delta V_o} \quad (5)$$

where, P_o is the output power from ACF converter and ΔV_o is the output voltage ripple.

2.4 Design of IACF Converter

The interleaved structure is used in which two Flyback converters are interleaved. Using interleaved technologies, the conduction loss of each switch is minimized, and reliability is improved because the ripple current of capacitors is reduced. The active clamp technique is adopted to recycle the leakage energy and to suppress the turn-off voltage spikes on the converter switches. The switching loss of the main switch is reduced because the switch operates with soft switching [34, 35]. The proposed IACF design [35] is adopted, where it was designed for PV system connected to a grid (AC output voltage). We have modified proposed IACF design for DC output (for powering loads and charging batteries) so the MOSFET rectifier is attained to achieve this objective. In this proposed IACF system, using a MOSFET bridge rectifier enables power losses to be minimized and efficiency levels to be improved, although at the expense of additional complexity in comparison of a diode bridge rectifier [37].

Fig. 3 shows the proposed IACF converter for a PV system with a bridge MOSFET rectifier. The proposed system consists of the PV module (that is represented as V_{in}), converter stage, inverter stage, L-C filters, and a rectifier. In the converter stage, two ACF including the main switches (S_{P1}, S_{p2}), the auxiliary switches (S_{a1}, S_{a2}), clamp capacitors (C_{C1}, C_{C2}), magnetic inductors (L_{m1}, L_{m2}) and diodes (D_{s1}, D_{s2}). In the inverter stage, the unfolding bridge composed of four switches (S_{s1}, S_{s2}, S_{s3}, and S_{s4}) operates at 50 Hz. The L-C filters include these inductors and capacitors (L_{f1}, L_{f2}, C_{f1}, and C_{f2}). The rectifier includes four switches (S_{r1}, S_{r2}, S_{r3}, and S_{r4}) based on N-MOSFET. Two 180° out-of-phase gate signals with the same duty cycle are applied to the main switches S_{P1} and S_{P2}. The gate signals of the active clamp switches S_{a1} & S_{a2} are applied during a very short time because of reducing the conduction loss of the active clamp switches [35]. This IACF design has twelve switches in total, as shown in Fig. 3.

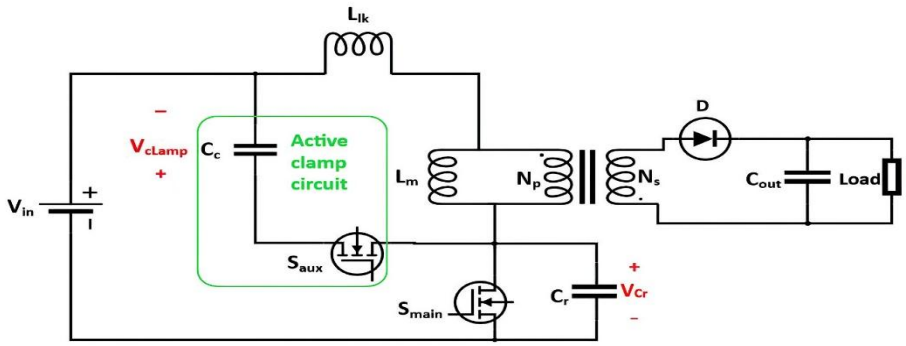

Fig. 2. Circuit configuration of ACF converter

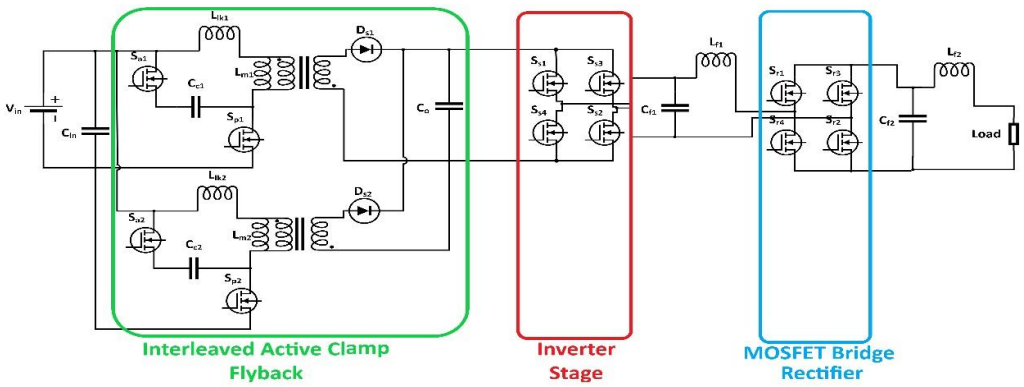

Fig. 3. IACF converter using the MOSFET bridge rectifier

2.5 Design of PID Controller and FLC

This section illustrates the linear and nonlinear controller that are PID controller and FLC, respectively. These proposed control systems are used to regulate the output of ACF converters with respect to the load requirements. Because the proposed IACF DC-DC converter has four main switches beside the inverter and rectifier, which requires complex controller systems for the 12 total switches. The output of these controller is pulse width modulation (PWM) for the MOSFETs (switches).

PID Controllers are everywhere due to its simplicity and excellent if not optimal performance in many applications. PID contains three proportional gain (K_P), integral gain (K_I), and derivative gain (K_D). The PID gains are used to decrease the rise time, eliminate the steady-state error, reduce the overshoot, settling time, and create more stability [38]. Table 1 shows the effect of the PID gains for the output response. In this paper, the output signals of the PID controller ($u(t)$) of the ACF are compared with a sawtooth signal to output square pulses (PWM) for the switch. The reference signal of the system is set to 24 V. Table 1 was used to tune the PID gains. It is found that the proposed ACF system is stable because of the range of damping factor ζ from 0 to 1 (the value is obtained by auto-tunning PID controller in MATLAB library) and having negative poles (in the left plane). The K_D gain is neglected, where the PI controller achieves a faster response than using the derivative gain because of its sluggish response [38-39].

Fuzzy Logic is a control system which controls nonlinear systems. FLC involves the processes of fuzzification, inference (decision making), and defuzzification [39]. The FLC converts the crisp error and its rate of change fuzzy variables that are mapped into linguistic labels. Membership functions are defined and associated with linguistic label for the input and output signals. Table 2 presents the rules of the FLC, the entries are the different fuzzy input sets for error (E) and change of error (E^*), and the cells are the corresponding fuzzy output sets for change of plant input. Five linguistic variables are combined for rules of FLC, where NL (Negative Large), NS (Negative Small), Z (Zero), PS (Positive Small), and PL (Positive Large). There are many different membership profiles for the FLC systems, Triangular profile is used for the DC-DC converters. Fig. 4 shows the surface view of FLC rules which are used to control the ACF, which shows nonlinearity mapping of the input and output signals.

3. SIMULATION RESULTS

This section describes the simulation results of MATLAB/SIMULINK. The input voltage (V_{in}) is set to 17 V (as the output of a solar panel), and these power converters are designed to provide 24 V (V_o). The reference voltage is set to 24 V for the closed loop control systems. The following subsections illustrate simulation results of the open loop system (no feedback system) for ACF and IACF converters, and closed loop control systems using PID and FLC for ACF converter only.

Table 1. Effects of changing PID parameters

Gain	Rise time	Overshoot	Settling time	Steady-State error	Stability
K_P	Decrease	Increase	Small change	Decrease	Degrade
K_I	Decrease	Increase	Increase	Eliminate	Degrade
K_D	Minor change	Decrease	Decrease	No effect	Improve

Table 2. Rules of FLC

E / E*	NL	NS	Z	PS	PL
NL	NL	NL	NS	NS	Z
Z	NS	NS	Z	PS	PS
PS	NS	Z	PS	PS	PL
PL	Z	PS	PS	PL	PL

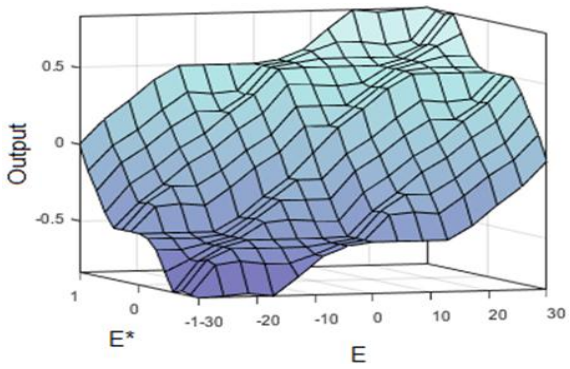

Fig. 4. Surface view of FLC rules

3.1 Open Loop Results

The derived equations in Section 4.1 were used to calculate the component values to achieve 24 V output voltage from a solar panel 17 V (V_{in}). The main parameters of the ACF & IACF designs are listed in Table 3, the parameters of IACF are obtained from [35], whereas the transformer ratio is recalculated for the required output response. The proposed ACF and IACF system are designed and modeled using MATLAB / SIMULINK to output 24 V_{DC} for the load requirements for DC-DC power converters.

3.2 ACF Design

Fig. 5 (a) shows the output voltage of the ACF design which stabilizes over 8 milliseconds. The peak-to-peak ripple is 12 mV, as shown in Fig. 5 (b). A 317 Ω is used as a resistive load, which results to output current equals 75.7 mA_{RMS} and the peak-to-peak ripple is 40 μA. The system efficiency of the ACF design is 88%, as the input & output power values are 2.02 and 1.815 W, respectively. The gate signal of the S_{main} and the S_{aux} which are opposite to each other, otherwise the input power will be short circuit and the power converter will be damaged.

3.3 IACF Design

Fig. 6 shows the gate signals of the main switches Sp_1, Sp_2, and the active clamp switches Sa_1, Sa_2 which are driven complementarily with the main switches. These gate signals are 0-5 V to turn on & off the MOSFETs, which represented the output of the driver gate circuits. Fig. 7 illustrates the DC output (V_{co}, voltage across C_o) when there is no inverter attached, which the output is 28.4 V, not the required voltage (24 V). Fig. 8 shows the unstable V_{co} for the proposed IACF system when the inverter is attached and L-C filter & rectifier circuits are not attached. This unstable profile has oscillating voltage of 5 $V_{peak\text{-}to\text{-}peak}$ of 28 V_{RMS} with spike values (from 11.5 to 33.5 $V_{peak\text{-}to\text{-}peak}$) at 125 Hz. Fig. 9 shows the AC square output voltage (28 $V_{peak\text{-}to\text{-}peak}$) in the presence of the L-C filter, where the MOSFET rectifier is not connected. Fig. 10 shows the DC output voltage (24 V) with settling time is 15.5 milliseconds when the rectifier is connected. The ripple voltage is 50 mV and the current values 75 mA_{RMS} when a 317 Ω is used for load. The efficiency is 90.1%, where the input power is 2.02 W and the output power is 1.82 W. The main purpose of the MOSFET rectifier in IACF inverter model is to rectify the AC output to DC profile for feeding DC loads and charging batteries, where the adopted IACF system was used to generate 220 V_{AC} to provide power to the grid [30, 35].

3.4 Closed Loop Results

This section illustrates the simulation results using closed loop control system. Two control systems are developed to control the output voltage of the ACF. Because the proposed IACF DC-DC power converter has 12 switches including the switches in the inverter and full-bridge rectifier. This requires complex control systems to control the sub-systems of the IACF DC-DC converter. Therefore, this work focuses on designing the control systems for the ACF DC-DC converters, where the performance analysis of these systems is conducted as follows.

3.5 PID of ACF

The system was simulated when the input voltage was constant and varying at different values. Fig. 11 (a) shows the output voltage of ACF converter with no overshoot when the input voltage is 17 V, which stabilizes after 7.5 milliseconds. The peak-to-peak ripple is 12 mV.

The output current equals 75.7 mA_{RMS} and its peak-to-peak ripple is 40 μA. The PV system is simulated using a variant input source, which mimics the output voltage from the harvested power from a solar panel. This harvested power would be changing with respect to solar radiation levels and other variables. The input voltage (V_{in}) is set to 16, 20, 25, 30, and 35 at 0, 0.01, 0.02, 0.03 and 0.04 milliseconds, respectively. The control system compensates these changes by adjusting the duty cycle. The maximum overvoltage and settling time happen when the input voltage changes to 20 V, as shown in Fig. 11 (b).

Table 3. Main parameters design of converters

Symbol	Parameter	ACF Value	IACF Value	Unit
V_{in}	Input voltage	17	17	V_{DC}
C_{in}	Input capacitance	-	13.2	*m*F
V_o	Output voltage	24	24	V_{DC}
n	Transformation turns ratio	17:35	1:1.66	-
L_m	Magnetizing inductance	524	10	μH
L_{lk}	Leakage inductor	17	0.12	μH
C_c	Clamp capacitor	0.15	0.3	μF
C_r	Resonance capacitor	1.5	-	*n*F
C_o	Output capacitance	25	0.15	μF
f_{sw}	Switching frequency	100	50	*k*Hz
f_b	Unfolding bridge frequency	-	50	Hz

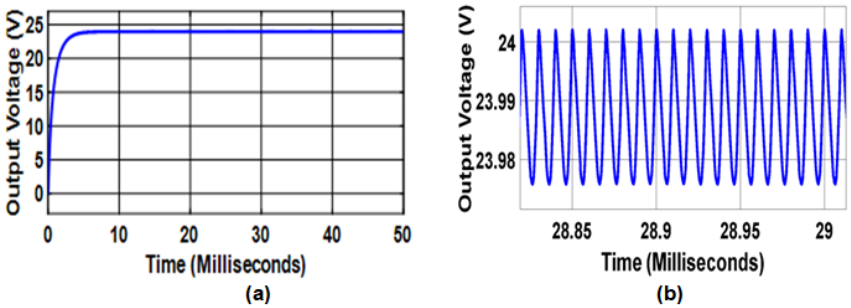

Fig. 5. Output response of ACF converter as open loop; (a) output voltage (b) peak to peak ripples

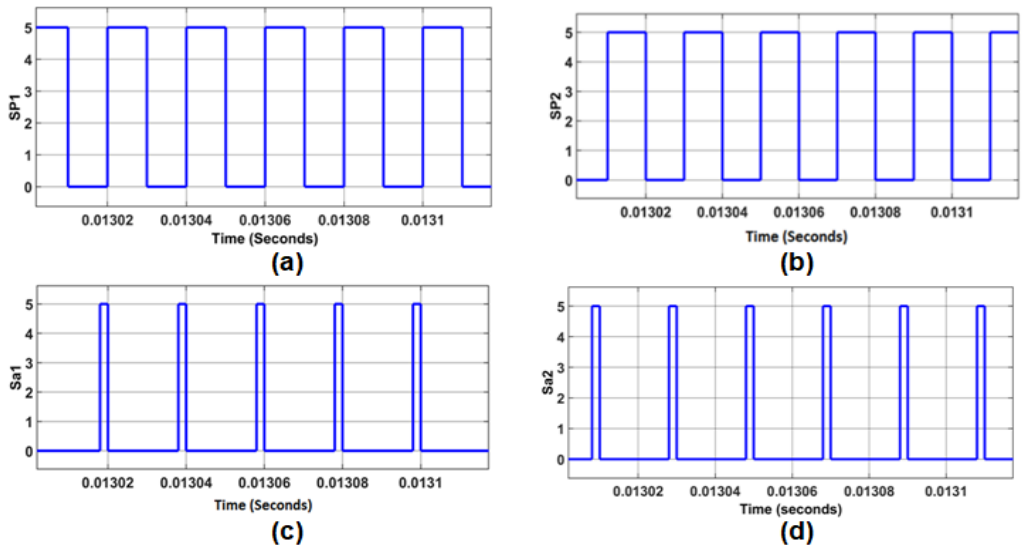

Fig. 6. Gate signal of switches; (a) sp_1, (b) sp_2, (c) sa_1, and (d) sa_2

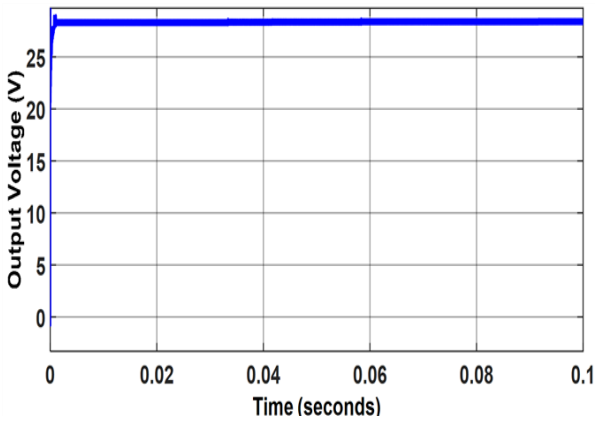

Fig. 7. Output voltage of C_o before when the inverter is attached

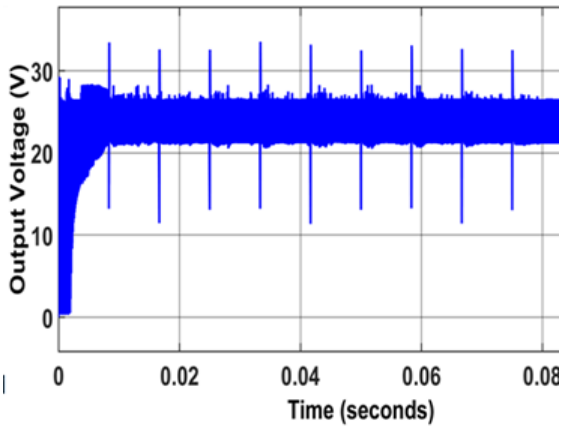

Fig. 8. Output voltage of $C_o$at proposed IACF DC-DC converter

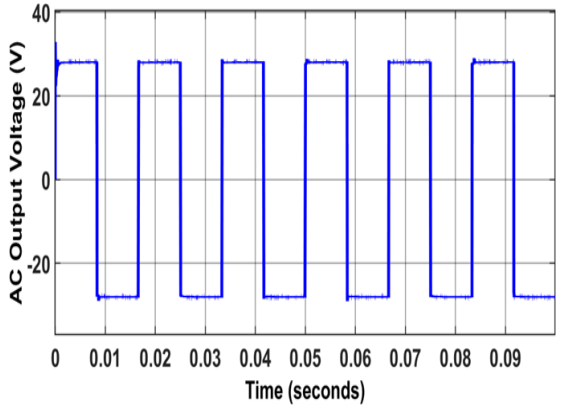

Fig. 9. AC output voltage

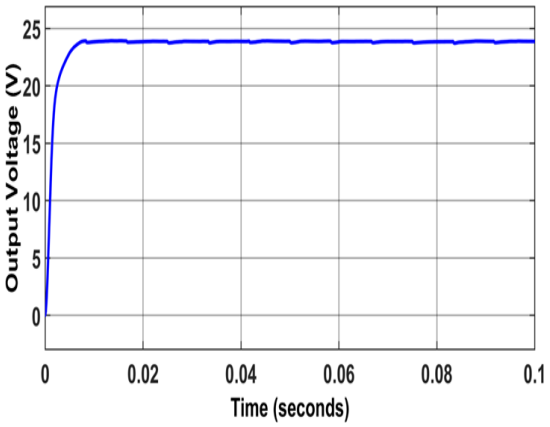

Fig. 10. DC output voltage

3.6 FLC of ACF

The output voltage of ACF converter using FLC stabilizes over 2.3 milliseconds for the fixed 17 V_{in} with no ripple voltage, as shown in Fig. 12 (a). The output voltage is stable at 24 V with no overvoltage while the V_{in} is varying at different times for the same conditions of the previous PID simulation setups, as illustrated in Fig. 12 (b). The simulation results of FLC shows better performance than PI controller, as discussed in the following section.

4. DISCUSSION

In this work, the performance of the proposed converters ACF & IACF were studied for PV system to output 24 V_{DC}. Through these studies, the advantages and disadvantages of each of the proposed converters are revealed. It is found that the advantages of ACF are single-ended topology, used for low voltage, and low power applications. The EMI is improved by the ZVS technique; however, it requires high switching frequency results to increasing the switching losses that can be mitigated by introducing the delay time to active the clamping operation. This leads to less efficiency of the ACF than the conventional Flyback converter [32-33]. The proposed IACF is more efficient than ACF, as shown in Section 5.1 (open loop performance), where the IACF alleviates the reverse-recovery problem for the secondary output diodes. Beside the aforementioned great benefits of the IACF converters makes it easier to create a central form of PV converter. The frequency of the ripple components at the waveforms is enhanced in relation to the number of interleaved converters, which is an additional advantage of interleaving. This feature provides a fast ripple component filtering or the use of smaller filtering elements. The potential to reduce the size of passive components is advantageous for cost reduction and having a portable converter. On the other

hand, the main disadvantages of the proposed IACF are high number of switches and slower response than the ACF, which requires complex control systems [33, 40].

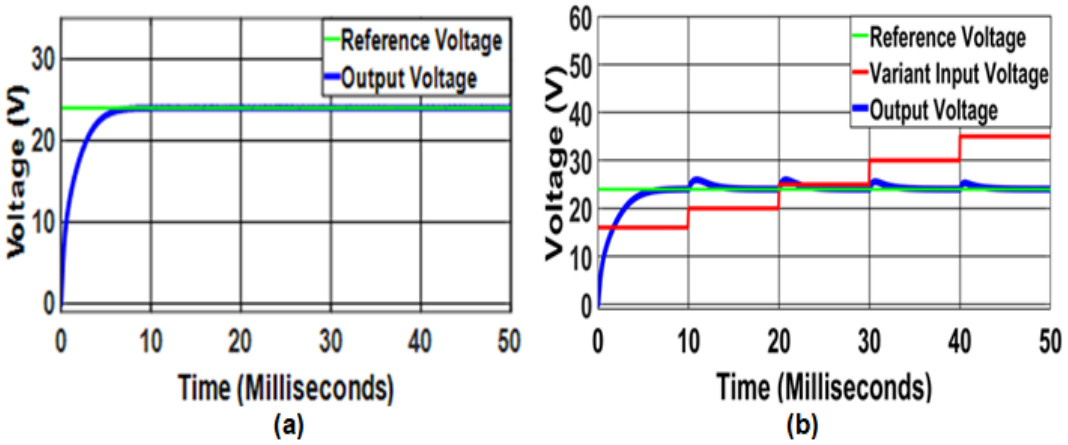

Fig. 11. Output voltage of ACF using PID for; (a) a constant V_{in} & (b) variant V_{in}

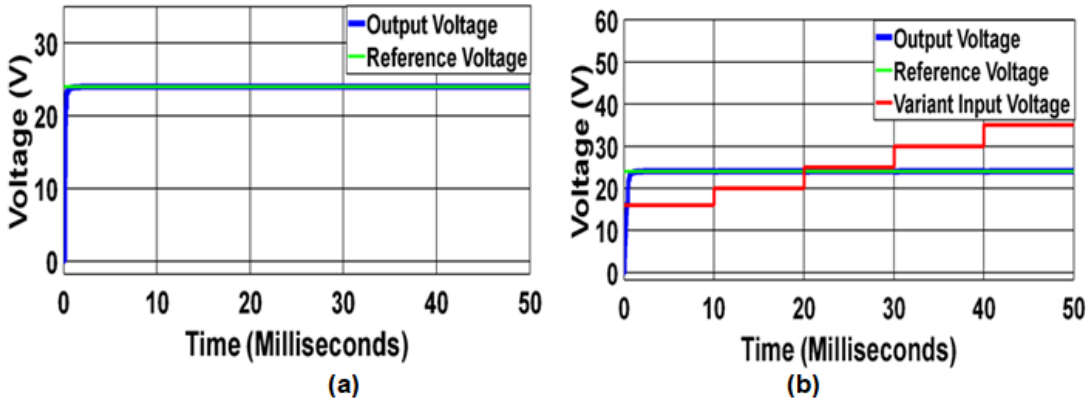

Fig. 12. Output voltage of ACF using FLC for; (a) a constant V_{in} & (b) variant V_{in}

For the same load (317 Ω), the output power values of the proposed converters ACF and IACF are almost same (1.815 W – 1.82 W, respectively) as the current is 75 mA_{RMS}. The ACF was controlled using PID control and FLC that improve the performance of the proposed ACF in comparison of the open loop system performance. The output power and system efficiency of the ACF using PI controller are similar to the open loop response. The main benefit of the PI (linear) controller is to regulate the output voltage to the required voltage; although the PV system experienced ripple and overshoot response when the input voltage (V_{in}) changes according to the sun radiation level or other parameters. The FLC achieved very small output ripple voltage (almost zero) and the output voltage was stable to 24 V while the input voltage was changing, as shown in Figs. 11&12. This is due to the nonlinearity of the FLC that achieves better performance for the ACF converter (nonlinear model) than the linear control system (PI controller).

5. CONCLUSION

This paper has presented advantages and disadvantages of different Flyback topologies. This work analyzed and discussed the performance of DC-DC ACF and IACF converters for solar power applications, which are suitable for low EMI applications. These DC-DC Flyback converters are designed to outputs 24 V_{DC} from 17 V (output voltage from a solar panel). MATLAB/SIMULINK was used to model and simulate the design of DC-DC ACF and IACF converters, where open loop and closed loop (PID/FLC) control systems are simulated according to operation and mathematical equations under various conditions. The PID & FLC control systems were used to regulate the output of ACF converters with respect to the load

requirements. This is due to high number of the switches in the proposed IACF DC-DC converter that has four main switches in addition to the switches of the inverter and rectifier. This requires complex control systems to compensate the voltage change from the the solar panel. The simulation results showed that the maximum efficiency was 90% for the IACF that is higher than ACF by 2%. The system response using FLC exhibited better performance than the PI controller when the input voltage was changing from the sun radiation level because of the nonlinearity behavior of the converters.

CONFLICT OF INTEREST STATEMENT

The technology, products, views, and opinions expressed by the author are solely theirs, and are in no manner associated with, endorsed by, or attributable to Genesis Robotics and Motion Technologies, LP, or its affiliates.

COMPETING INTERESTS

Authors have declared that no competing interests exist.

REFERENCES

1. Masoum MAS, Badejani SMM, Fuchs EF. Microprocessor-controlled new class of optimal battery chargers for photovoltaic applications. IEEE Transactions on Energy Conversion. 2004; 19(3):599-606.
2. Fakhry M, Saber M, Eltantawi ME, Kaddah SS, Badr BM. Design and Analysis of Controller SEPIC and LLC Converters for Photovoltaic Systems. International Journal of Engineering Applied Sciences and Technology. 2020;5(8):54-63.
3. Tanaka K, Sakoguchi E, Fukuda Y, Takeoka A, Tokizaki H. Residential solar powered air conditioner. Proc. Eur. Power Electronics Conf. 1993:127-132.
4. Magdy M, Hamouda A, Kaddah SS, Badr BM. Design Control Systems for Buck-Boost and Cuk Converters for Solar Power Applications. International Journal of Scientific & Engineering Research. 2021;15(2):556-563.
5. Mammano AR. Fundamentals of Power Supply Design. Texas Instruments;2017.
6. McLyman CWT. Transformer and Inductor design Handbook. 2nd ed, Marcel Dekker; 1988.
7. Ashraf Y, Elsobky NE, Hamouda MA, Sabry M, Kaddah SS, Badr BM. Controlling Single-Stage and Quasi-Resonant Flyback converters for solar power systems. Jordan Journal of Electrical Engineering, 2021; 7(2): 148-165.
8. Chandhaket S, Ogura K, Nakaoka M, Konishi Y. High-Frequency Flyback Transformer Linked Utility-Connected Sinewave Soft-Switching Power Conditioner using a Switched Capacitor Snubber," The 4th International Power Electronics and Motion Control Conference, Xi'an, China, 2004;3:1242-1247.
9. Wang D. Analysis, Design and Implementation of an Active Clamp Flyback converter. International Conference on Power Electronics and Drives Systems. 2005;424-429.
10. Lin BR, Huang CE, Huang K, Wang D. Design and implementation of zero voltage switching Flyback Converter with Synchronous Rectifier. IEEE Proceedings - Electric Power Applications, 2006;153 (3):420-429.
11. Abramovitz A, Liao C, Smedley K. State-plane analysis of regenerative snubber for flyback converters. IEEE Transactions on Power Electronics. 2013;28(11):5323-5332.
12. Sperb JD, Zanatta IX, Michels L, Rech C, Mezaroba M. Regenerative Undeland Snubber Using a ZVS PWM DC–DC Auxiliary Converter Applied to Three-Phase Voltage-Fed Inverters. IEEE Transactions on Industrial Electronics. 2011;58(8):3298-3307.
13. Bauman J, Kazerani M. A Novel Capacitor-Switched Regenerative Snubber for DC/DC Boost Converters. IEEE Transactions on Industrial Electronics, 2011;58(2):514-523.
14. Ai TH. A novel integrated non dissipative snubber for flyback converter. International Conference on Systems & Signals. 2005;66-71.
15. Konishi Y, Huang YF. Soft-switching buck boost converter using pulse current regenerative resonant snubber. Electronics Letters. 2007;43(2):127-128.
16. Fleury P and Al-Haddad K. Universal input voltage, unity power factor, high efficiency flyback rectifier with regenerative snubber. Canadian Conference on Electrical and Computer Engineering, Saskatoon, SK, Canada. 2005;595-598.
17. Abramovitz A, Cheng T, Smedley K. Analysis and Design of Forward Converter

with Energy Regenerative Snubber. IEEE Transactions on Power Electronics, 2010;25(3):667-676.
18. Matsushita A, Tai H, Yasuoka I, Matsumoto T. Inverter circuit with the regenerative passive snubber. Power Conversion Conference, Nagoya, Japan. 2007;167-171.
19. Jovanovic MM, Hopkins DC, Lee FC. Evaluation and design of megahertz-frequency off-line zero-current-switching quasi-resonant converters. IEEE Transactions on Power Electronics. 1989;4(1):136-146.
20. Mo Q, Chen M, Zhang Z, Zhang Y, Qian Z. Digitally controlled active clamp interleaved flyback converters for improving efficiency in photovoltaic grid-connected micro-inverter. Twenty-Seventh Annual IEEE Applied Power Electronics Conference and Exposition (APEC), Orlando, FL, USA. 2012;555-562.
21. Huang G, Liang T, Chen K. Losses analysis and low standby losses quasi-resonant flyback converter design. IEEE International Symposium on Circuits and Systems (ISCAS), Seoul, Korea (South). 2012;217-220.
22. Zhang MT, Jovanovic MM, Lee FCY. Design considerations and performance evaluations of synchronous rectification in flyback converters. IEEE Transactions on Power Electronics.1998; 13(3):538-546.
23. Tabisz WA, Gradzki P, Lee FC. Zero-voltage-switched quasi-resonant buck and flyback converters Experimental results at 10 MHz. IEEE Power Electronics Specialists Conference, Blacksburg, VA, USA. 1987;404-413.
24. Watson R, Lee FC, Hua GC. Utilization of an active-clamp circuit to achieve soft switching in flyback converters. IEEE Transactions on Power Electronics, 1996;11(1):162-169.
25. Lin KH, Lee FC. Zero-Voltage-Switching Techniques in DC/DC Converter. IEEE;1990.
26. Ridley RB, Tabisz WA, Lee FCY, Vorperian V. Multi-loop control for quasi-resonant converters. IEEE Transactions on Power Electronics, 1991;6(1):28-38.
27. Tibola G, Lemmen E, Duarte JL, Barbi I. Passive regenerative and dissipative snubber cells for isolated SEPIC converters: Analysis, design, and comparison. IEEE Transactions on Power Electronics. 2017;32(12):9210-9222.
28. Tamyurek B, Kirimer B. An interleaved high-power flyback inverter for photovoltaic applications. IEEE Transactions Power Electronics,2014;30(6):3228-3241.
29. Lindstrom EO, Rodriguez LAG, Oliva AR, Balda JC. A novel method to compare converters for PV applications based on energy efficiency. In Argentine Conference on Micro-Nanoelectronics, Technology and Applications (EAMTA), IEEE. 2014;24-28.
30. Quesada DP. Design and construction of an isolated DC-DC flyback converter for solar MPPT purposes. Senior Thesis in Electrical Engineering, University of Illinois at Urbana-Champaign;2018.
31. Sharma A, Singh S. Flyback-Forward Converter for Solar Based Application. International Journal of Advanced Research in Electrical, Electronics and Instrumentation Engineering. 2016; 5(5):3600-3607.
32. Suskis P, Galkin I, Zakis J. Design and Implementation of Flyback MPPT Converter for PV-Applications. Electric Power Quality and Supply Reliability Conference (PQ), Estonia, Rakvere, 2014;291-296.
33. Anandakumar V, Ramesh A, Mariappane E. Implementation of New Control Technique for Interleaved Flyback Inverter Based PV System. International Journal of Engineering Research & Technology (IJERT), 2014;3(2):1151-1156.
34. Deshpande SG, Bhasme N. Modeling and Simulation of Microinverter with Flyback Converter for grid connected PV systems.International Journal of Electrical and Electronics Engineering Research (IJEEER), 2017;7(4):71-82.
35. Kim YH, Kim JH, Won CY, Jung YC, Lee WT. Soft switching interleaved active clamp Flyback inverter for a photovoltaic AC module system. IEEE Proceedings of the 14th European Conference on Power Electronics and Applications. Birmingham, United Kingdom. 2011;1-9.
36. Lin BR, Chiang HK, Chen KC, Wang D. Analysis, design and implementation of an active clamp flyback converter. International Conference on Power Electronics and Drives Systems, IEEE, Kuala Lumpur, Malaysia, 2005;1:424-429.
37. Sevel B, *MOSFETs:* Increased Efficiency in Bridge Rectifiers. EDN;2007. Available:https://www.edn.com/mosfets-increased-efficiency-in-bridge-rectifiers/

38. Badr BM, Ali WG. Nanopositioning Fuzzy Control for Piezoelectric Actuators. International Journal of Engineering & Technology, 2010;10(1):50-54.
39. Badr BM, Ali WG. Fuzzy Control for Nanopositioning Piezoelectric Actuators. VDM Verlag; 2011.
40. Tamyurek B, Torrey DA. A three-phase unity power factor single-stage AC–DC converter based on an interleaved flyback topology. IEEE Trans. Power Electron, 2011;26(1):308–318.

Peer-review history:
The peer review history for this paper can be accessed here:
http://www.sdiarticle4.com/review-history/69966